

Selective Classification Via Neural Network Training Dynamics

Stephan Rabanser

University of Toronto & Vector Institute
stephan@cs.toronto.edu

Anvith Thudi

University of Toronto & Vector Institute
anvith.thudi@mail.utoronto.ca

Kimia Hamidieh

University of Toronto & Vector Institute
kimia@cs.toronto.edu

Adam Dziedzic

University of Toronto & Vector Institute
ady@vectorinstitute.ai

Nicolas Papernot

University of Toronto & Vector Institute
nicolas.papernot@utoronto.ca

Abstract

Selective classification is the task of rejecting inputs a model would predict incorrectly on through a trade-off between input space coverage and model accuracy. Current methods for selective classification impose constraints on either the model architecture or the loss function; this inhibits their usage in practice. In contrast to prior work, we show that state-of-the-art selective classification performance can be attained solely from studying the (discretized) training dynamics of a model. We propose a general framework that, for a given test input, monitors metrics capturing the disagreement with the final predicted label over intermediate models obtained during training; we then reject data points exhibiting too much disagreement at late stages in training. In particular, we instantiate a method that tracks when the label predicted during training stops disagreeing with the final predicted label. Our experimental evaluation shows that our method achieves state-of-the-art accuracy/coverage trade-offs on typical selective classification benchmarks.

1 Introduction

Machine learning (ML) is increasingly deployed in high-stakes decision-making environments, where it is critical to detect inputs that the model could misclassify. This is particularly true when deploying deep neural networks (DNNs) for applications with low tolerances for false-positives (i.e., classifying with a wrong label), such as healthcare (Challen et al., 2019; Mozannar and Sontag, 2020), self-driving (Ghodsi et al., 2021), and law (Vieira et al., 2021). This problem setup is captured by the selective classification (SC) framework, which introduces a gating mechanism to abstain from predicting on individual test points (Geifman and El-Yaniv, 2017). Specifically, SC aims to (i) only accept inputs on which the ML model would achieve high accuracy, while (ii) maintaining high coverage, i.e., accepting as many inputs as possible.

Current state-of-the-art selective classification techniques take one of two directions: the first augments the architecture of the underlying ML model (Geifman and El-Yaniv, 2019); the second trains the model using a purposefully adapted loss function (Gangrade et al., 2021). The unifying principle behind these methods is to modify the training stage in order to accommodate selective classification. This lack of practicality hinders the adoption of selective classification. In this work, we instead show that these modifications are unnecessary to attain state-of-the-art selective classification performance.

We present the first framework for selective classification based on neural network training dynamics (see Figure 1). Typical DNNs are trained sequentially e.g., using stochastic gradient descent. Hence, as training goes on, the optimization process yields a sequence of intermediate models. These models, in particular their predictions on a given test point, can then be used to construct a threshold-able score

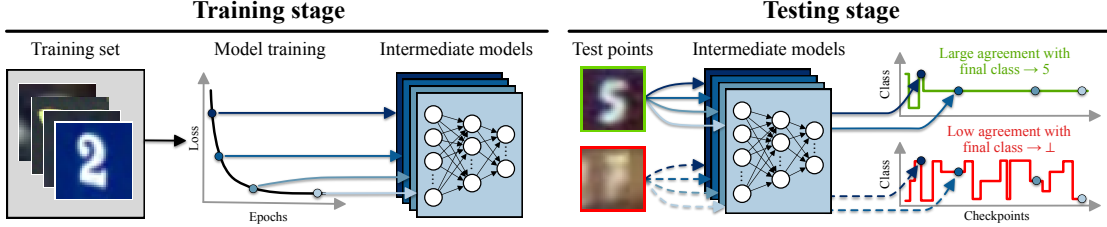


Figure 1: **Our proposed NNTD method.** During the model training stage, we store checkpoints of intermediate models. At inference time, given a test input, we compute various metrics capturing the agreement of intermediate predictions with the final model prediction. Data points with high agreement are accepted while data points with low agreement are rejected.

for selective classification. Intuitively, if we understood defining traits of the intermediate predictions for correctly classified points, we can define a gating mechanisms to reject incorrectly classified points.

Through an analysis of neural network training dynamics, we first observe that an important property of the intermediate predictions is to assess if they agree with the final prediction. To that end, we introduce a set of assumptions on how the expected disagreement evolves during training for correctly classified points, alongside the variance of this disagreement. Using these assumptions, we can upper-bound the probability that the test point is correctly classified given its intermediate predictions. Verifying these assumptions empirically, we observe that the expected disagreement is almost always 0 (except initially) for correctly classified points, and the variance decreases in a convex manner.

These observations lead to our first proposed method, which imposes a threshold on the last intermediate model whose prediction disagrees with the final label prediction. Noting however the potential for noise inherent in training (and hence the intermediate models’ predictions) to hamper the effectiveness of this method, we propose an improved method which thresholds a biased average based on multiple intermediate models disagreeing with the final label prediction. The latter method improves on state-of-the-art (SOTA) accuracy/coverage trade-offs for selective classification.

Our main contributions are as follows:

1. We propose a novel method for SC based on neural network training dynamics (dubbed NNTD) in which we devise an effective scoring mechanism capturing label disagreement of intermediate models with the final prediction for a particular test point.
2. We theoretically motivate the benefits of NNTD by deriving an upper-bound on the probability of a test point being correctly classified.
3. We perform a comprehensive set of empirical experiments on established SC benchmarks. Our results obtained with NNTD demonstrate a highly favorable accuracy/coverage of NNTD-based selective classification, especially at low false-positive rates.

2 Background

Our work considers the standard supervised multi-class classification setup. We assume to have access to a dataset $D = \{(\mathbf{x}_i, y_i)\}_{i=1}^M$ consisting of data points (\mathbf{x}, y) with $\mathbf{x} \in \mathcal{X}$ and $y \in \mathcal{Y}$. We refer to $\mathcal{X} = \mathbb{R}^d$ as the covariate space of dimensionality d and $\mathcal{Y} = \{1, 2, \dots, C\}$ as the label space consisting of C classes. All data points (\mathbf{x}, y) are sampled independently from the underlying distribution p defined over $\mathcal{X} \times \mathcal{Y}$. Our goal is to learn a prediction function $f : \mathcal{X} \rightarrow \mathcal{Y}$ which minimizes the classification risk with respect to the underlying data distribution p and an appropriately chosen loss function $\ell : \mathcal{Y} \times \mathcal{Y} \rightarrow \mathbb{R}$.

2.1 Selective Classification

Setup Selective classification alters the standard classification setup by introducing a rejection class \perp through a *gating mechanism* (El-Yaniv and Wiener, 2010). In particular, a selective prediction model

introduces a selection function $g : \mathcal{X} \rightarrow \mathbb{R}$ which determines if a model should predict on a data point \mathbf{x} . Given an acceptance threshold τ , the resulting predictive model can be summarized as follows:

$$(f, g)(\mathbf{x}) = \begin{cases} f(\mathbf{x}) & g(\mathbf{x}) \geq \tau \\ \perp & \text{otherwise.} \end{cases} \quad (1)$$

Evaluation Metrics Prior work evaluates the performance of a selective classifier (f, g) based on two metrics: the *coverage* of (f, g) (i.e., what fraction of points we predict on) and the selective *accuracy* of (f, g) on the points it accepts. Successful SC methods aim at obtaining both high accuracy and high coverage. Note that these two metrics are at odds with each other: naïvely increasing accuracy leads to lower coverage and vice-versa. The complete performance profile of a model can be specified using the risk-coverage curve, which defines the risk as a function of coverage (El-Yaniv and Wiener, 2010). These metrics can be formally defined as follows:

$$\text{cov}(f, g) = \frac{|\{\mathbf{x} : g(\mathbf{x}) \geq \tau\}|}{|D|} \quad \text{acc}(f, g) = \frac{|\{\mathbf{x} : f(\mathbf{x}) = y, g(\mathbf{x}) \geq \tau\}|}{|\{\mathbf{x} : g(\mathbf{x}) \geq \tau\}|} \quad (2)$$

2.2 Related Work

Selective Classification The first work on SC in the context of deep neural networks (DNNs) is the softmax response (SR) mechanism (Geifman and El-Yaniv, 2017). A threshold τ is applied to the maximum response of the softmax layer $\max_{y \in \mathcal{Y}} f(y|\mathbf{x})$. Given a confidence parameter δ and desired risk r^* , this creates a selective classifier (f, g) whose test error is no larger than r^* with probability of at least $1 - \delta$. It was further shown by Lakshminarayanan et al. (2017) that model ensembles can improve upon the basic SR method. In our work, we leverage intermediate models yielded during training to avoid the costly training of separate models to obtain an ensemble. A similar approach leveraging intermediate predictions is given by Huang et al. (2020) where intermediate prediction are incorporated into the loss function during training. As opposed to ensemble approaches, SelectiveNet (SN) (Geifman and El-Yaniv, 2019) trains a model to jointly optimize for classification and rejection. A penalty is added to the loss to enforce a coverage constraint using a variant of the interior point method. In a different approach, Deep Gamblers (DG) (Liu et al., 2019) transform the original C -class classification problem into a $(C+1)$ -class problem where the $(C+1)$ -th class represents model abstention. This introduces less architectural changes than SelectiveNet but still involves a different training procedure. Recently, One-Sided Prediction (OSP) (Gangrade et al., 2021) has proposed to learn disjoint classification regions corresponding to each class; rejection is then implicitly defined as the gap between these regions via a constrained learning problem. Other similar approaches include: abstention based on the variance statistics from several dropout-enabled forward passes (Gal and Ghahramani, 2016), performing statistical inference for the marginal prediction-set coverage rates using model ensembles (Feng et al., 2021), confidence prediction using an earlier snapshot of the model (Geifman et al., 2018), and complete precision for SC via classifying only when models consistent with the training data predict the same output (Khani et al., 2016).

Example Difficulty A related line of work is identifying *difficult* examples, or how well a model can generalize to a given unseen example. Jiang et al. (2020) introduce a per-instance empirical consistency score which estimates the probability of predicting the ground truth label with models trained on data subsamples of different sizes. Unlike our approach, however, this requires training a large number of models. Toneva et al. (2018) quantifies example difficulty through the lens of a forgetting event, in which the example is misclassified after being correctly classified. However, the metrics that we introduce in § 3, are based on the disagreement of the label at each checkpoint with the final predicted label. Other approaches estimate the example difficulty by: prediction depth of the first layer at which a k -NN classifier correctly classifies an example (Baldock et al., 2021), the impact of pruning on model predictions of the example (Hooker et al., 2019), and estimating the leave-one-out influence of each training example on the accuracy of an algorithm by using influence functions (Feldman and Zhang, 2020). Closest to our method, the work of Agarwal et al. (2020) utilizes gradients of intermediate models during training to rank examples by difficulty. In particular, they average pixel-wise variance of gradients for each given input image. Notably, this approach is more

costly and less practical than our approach and also does not study the accuracy/coverage trade-off which is of paramount importance to SC.

3 Our Method

We now introduce our selective classification algorithms based on neural network training dynamics. We refer to this class of methods as NNTD. These methods are motivated by a theoretical framework that links parameters characterizing training dynamics (e.g., how predictions evolve during training) to the goal of predicting the likelihood of a point being correctly classified.

3.1 A Framework for Rejection

We first build some intuition as to how having access to intermediate states of the model during training can inform our gating mechanism. That is, how training dynamics can help us decide when to abstain from predicting on an input. To do so, we introduce a bound on the probability of a datapoint being correctly classified based on the predictions intermediate models gave on that datapoint.

Let us denote the test dataset as \mathcal{D} . Given a model f , let $D' \subset \mathcal{D}$ be the subset which f correctly classifies. We are interested in the setting where f is trained sequentially (e.g., with stochastic gradient descent). We thus also have access to a sequence of T intermediate states for f , which we denote $\{f_1, \dots, f_T\}$. In this sequence, note that f_T is exactly the final model f .

Now, let p_t represent the random variable for outputs on D' given by an intermediate model f_t where the outputs have been binarized: we have 0 if the output agrees with the final (correct) prediction and 1 if not.¹ In other words, p_t is the distribution of labels given by first drawing $\mathbf{x} \sim D'$ and then outputting $1 - \delta_{f_t(\mathbf{x}), f_T(\mathbf{x})}$ where δ denotes the Dirac delta function. Here, \sim corresponds to sampling *w.r.t* some distribution on D' . For example, if all test points we evaluate our model on are taken from a larger finite set \mathcal{D} , then D' is also finite and so \sim can correspond to the uniform distribution on D' (as it is well-defined).

Note that we always have a well-defined mean and a well-defined variance for p_t as it is bounded. Furthermore, we always have the variances and expectations of $\{p_t\}$ converge to 0 with increasing t (as $p_T = 0$ always and the sequence is finite). To state this formally, let $v_t = \mathbb{V}[p_t]$ and $e_t = \mathbb{E}[p_t]$ denote the variances and expectations over correctly classified points. Note that $e_T, v_T = 0$, so both e_t and v_t converge²

However, the core problem is that we do not know how this convergence in the variance and expectation occurs. More specifically, if we knew the exact values of e_t and v_t , we could use the following bound on the probability of a particular data point being correctly classified. Note, we introduce the notation $\{a_1, \dots, a_T\}$ where $a_t = 1 - \delta_{f_t(\mathbf{x}), f_T(\mathbf{x})}$ which we call the "label disagreement (at t)", which we use later in the paper. Note that the a_t are constants defined with respect to any input, while p_t represent the distribution over a_t over all inputs in D' .

Lemma 1. *Given a datapoint \mathbf{x} , let $\{a_1, \dots, a_T\}$ where $a_t = 1 - \delta_{f_t(\mathbf{x}), f_T(\mathbf{x})}$. Assuming not all $a_t = e_t$ then the probability $\mathbf{x} \in D'$ is $\leq \min_{v_t \text{ s.t. } a_t \neq e_t} \frac{v_t}{|a_t - e_t|^2}$.*

Proof. By Chebyshev's inequality we have the probability of a particular sequence $\{a_1, \dots, a_T\}$ occurring is $\leq \frac{v_t}{|a_t - \mathbb{E}(p_t)|^2}$ for every t (a bound on any of the individual a_t occurring as that event is in the event $|p_t - e_t| \geq |a_t - e_t|$ occurs), and so taking the minimum over all these upper-bounds we obtain our upper-bound. \square

We do not guarantee Lemma 1 is tight. Though we do take a minimum to make it tighter, this is a minimum over inequalities all derived from Markov's inequality.³ Despite this potential looseness, using the bound from Lemma 1, we can design a naïve selective classification protocol; for a given input \mathbf{x} , if the

¹We note that f_t does not necessarily output the correct prediction on D' , only the final model f does.

²For all $\epsilon > 0$ there exists an $N \in \{1, \dots, T\}$ (i.e $N = T$) such that $v_t < \epsilon$ for all $t > N$. Similarly, for all $\epsilon > 0$ there exists a (possibly different) $N \in \{1, \dots, T\}$ such that $e_t < \epsilon$ for all $t > N$.

³One could potentially use information about the distribution of incorrectly classified datapoints to further refine this bound. Also recall that p_t is only defined over the correctly classified points.

upper-bound on the probability of being correct is lower than some threshold τ reject, else accept. However, as mentioned earlier, we have the following two problems preventing us from readily using this method:

1. What is $\mathbb{E}[p_t]$ during training on correctly classified points?
2. How does $\mathbb{V}[p_t]$ change during training?

These problems represent questions about how the predictions on correctly classified points evolve during training, i.e., the *training dynamics* of correctly classified points. More generally, they exemplify how a characterization of the training dynamics of correctly classified datapoints could be useful for selective classification. Informally, the first problem represents knowing how often we predict the true label at step t , and the second problem represents knowing how we become more consistent as we continue training.

The rest of this section will focus on the two methods we propose for selective classification. Although we do not give any formal guarantees of correctness for our methods, their design and assumptions are informed by Lemma 1 and by empirical estimates of e_t and v_t (later described in § 4.3).

3.2 The Minimum Score s_{\min}

In what follows we will, after two simplifying assumptions, derive a candidate selective classification algorithm based off of Lemma 1. It is worth remarking that, despite our method being given by a simplification of Lemma 1, the performance of our approach is not upper bounded by Lemma 1.

In § 4.3 we observe that the expected values for the p_t distribution from § 3.1, which we denote e_t , are near 0 for most t ; we will therefore further simplify our setup by assuming $e_t = 0$ for all t ⁴. Note that if $e_t = 0$ and the label disagreement $a_t = 1$, then $\frac{v_t}{[a_t - \mathbb{E}[p_t]]^2} = v_t$. Assuming $e_t = 0$ for all t , based on Lemma 1 the measure for acceptance we are interested in is $s_{\min} = \min_{t \text{ s.t. } a_t=1} v_t$. Note now s_{\min} depends on what v_t are. From § 4.3 we observe v_t monotonically decrease in a convex manner. Thus, we choose to approximate the empirical trend observed in § 4.3 with $v_t = 1 - t^k$ (for $k \in (0, 1]$), which also decrease in a convex manner. Later, we empirically determine which k is best for our methods.

Our first algorithm for selective classification is hence given by:

1. Denote $L = f_T(\mathbf{x})$, i.e. the label our final model predicts.
2. If $\exists t \text{ s.t. } a_t = 1$ then compute $s_{\min} = \min_{t \text{ s.t. } a_t=1} v_t$ as per the notation in § 3.1 (i.e $a_t = 1$ iff $f_t(x) \neq L$), else accept \mathbf{x} with prediction L .
3. If $s_{\min} > \tau$ accept \mathbf{x} with prediction L , else reject (\perp).

We note that the min score is similar to the hardness score proposed in [Sadeghzadeh et al. \(2021\)](#).

Intuitively, as all our candidate v_t decrease, the algorithm imposes a last intermediate model which can output a prediction that disagrees with the final prediction: hereafter, the algorithm must output models that consistently agree with the final prediction. The effectiveness of this method depends on how quickly v_t decrease (assuming $e_t = 0$ always) as opposed to the variance for incorrectly predicted data points. In particular, if there was an index N such that for $t > N$, we have that $f_t(x) = f_T(x)$ for correctly classified points, but never (or rarely) for incorrectly classified points, then this method would successfully separate the correct from the incorrect.

3.3 The Average Score s_{avg}

Note that the previous method, defined by the score s_{\min} could be sensitive to stochasticity in training and hence perform sub-optimally. In particular, this algorithm could be noisy for different training runs (of otherwise identical models) as $\min_{t \text{ s.t. } a_t=1} v_t$ could vary drastically based on the exact sequence of mini-batches used during training.

In light of this potential limitation we propose the following "averaging" algorithm:

1. Denote $L = f_T(\mathbf{x})$, i.e. the label our final model predicts.

⁴Later, in Appendix B.3.3 we consider removing this assumption and observe marginally worse results.

Table 1: **Performance at low target errors.** Our $\text{NNTD}(s_{\text{avg}}, 0.05)$ method either matches or provides higher coverage levels of the test set at a fixed target error than other competing methods. Bold entries are within one standard deviation of each other over 5 random runs (standard deviations are in Table 9).

Dataset	Target	NNTD		SAT		DG		SN		SR		MC-DO	
	Error	Cov \uparrow	Err	Cov \uparrow	Err	Cov \uparrow	Err	Cov \uparrow	Err	Cov \uparrow	Err	Cov \uparrow	Err
CIFAR-10	2%	91.2	1.99	90.3	1.97	89.1	2.02	88.3	2.03	85.8	1.98	86.1	2.01
	1%	86.4	1.00	86.1	1.02	85.5	1.03	84.4	0.98	79.1	1.01	79.9	1.01
	0.5%	75.9	0.49	76.0	0.51	75.2	0.51	74.7	0.49	71.2	0.51	72.0	0.50
SVHN	2%	98.5	1.98	98.2	1.99	97.8	2.06	97.7	2.03	97.6	1.99	97.9	2.00
	1%	96.3	0.99	95.7	1.03	94.8	0.99	94.5	1.04	93.5	1.01	94.1	0.97
	0.5%	88.1	0.50	87.9	0.51	86.4	0.51	86.0	0.51	70.0	0.50	70.1	0.49
Cats & Dogs	2%	97.7	2.01	98.2	1.98	98.0	2.03	97.4	1.98	95.1	1.99	95.7	1.99
	1%	93.1	1.01	93.6	0.98	92.6	0.97	92.2	0.98	86.9	0.98	88.6	1.01
	0.5%	85.7	0.51	86.0	0.49	85.3	0.49	84.8	0.46	68.4	0.48	70.1	0.51

Table 2: **Performance at high target coverage.** Similar as shown in Table 1, $\text{NNTD}(s_{\text{avg}}, 0.05)$ matches or outperforms state-of-the-art error rates at fixed coverage levels (standard deviations are in Table 10).

Dataset	Target	NNTD		SAT		DG		SN		SR		MC-DO	
	Coverage	Cov	Err \downarrow	Cov	Err \downarrow	Cov	Err \downarrow	Cov	Err \downarrow	Cov	Err \downarrow	Cov	Err \downarrow
CIFAR-10	100%	100	6.07	100	6.06	100	6.11	100	6.13	100	6.13	100	6.13
	95%	95.0	3.24	95.1	3.32	95.1	3.47	95.0	4.08	94.9	4.48	95.1	4.48
	90%	90.1	1.83	89.9	1.90	90.0	2.19	90.1	2.29	90.1	2.78	90.0	2.87
	80%	79.9	0.64	80.0	0.65	80.1	0.66	80.1	0.81	79.8	1.05	79.9	1.01
	70%	69.8	0.34	69.9	0.32	69.8	0.41	70.2	0.30	70.0	0.47	70.1	0.42
SVHN	100%	100	2.68	100	2.71	100	2.72	100	2.77	100	2.77	100	2.77
	95%	95.0	0.88	95.1	0.95	95.1	1.01	95.0	1.07	94.9	1.15	95.1	1.12
	90%	90.1	0.55	89.9	0.58	90.0	0.63	90.1	0.71	90.1	0.82	90.0	0.76
	80%	79.9	0.38	80.0	0.37	80.1	0.43	80.1	0.48	79.8	0.55	79.9	0.53
	70%	69.8	0.33	69.9	0.33	69.8	0.35	70.2	0.45	70.0	0.50	70.1	0.49
Cats & Dogs	100%	100	3.48	100	3.45	100	3.41	100	3.56	100	3.56	100	3.56
	95%	95.1	1.51	95.1	1.45	95.0	1.43	94.9	1.61	94.8	1.92	95.1	1.95
	90%	90.1	0.60	89.9	0.57	90.0	0.69	90.1	0.95	90.1	1.13	90.0	1.09
	80%	79.9	0.42	80.0	0.41	80.1	0.56	80.1	0.39	79.8	0.69	79.9	0.58
	70%	69.8	0.36	69.9	0.33	69.8	0.45	70.2	0.33	70.0	0.62	70.1	0.51

2. If $\exists t$ s.t. $a_t = 1$, compute $s_{\text{avg}} = \frac{\sum v_t a_t}{\sum a_t}$, else accept \mathbf{x} with prediction L .
3. If $s_{\text{avg}} > \tau$ accept \mathbf{x} with prediction L , else reject (\perp).

Intuitively, recalling our previous candidates for v_t , s_{avg} computes a weighted average, adding little weight to later disagreements with the final prediction (but still increasing the denominator by the same amount). As we demonstrate in § 4, this averaging procedure leads to considerably more robust results.

4 Empirical Evaluation

4.1 Setup

Datasets & Training We evaluate our proposed approach on image dataset benchmarks that are common in the selective classification literature: CIFAR-10/CIFAR-100 (Krizhevsky et al., 2009), SVHN (Netzer et al., 2011), Cats & Dogs⁵, and GTSRB (Houben et al., 2013). For each dataset, we train a deep neural network following the VGG16 architecture (Simonyan and Zisserman, 2014) (using batch normalization and dropout) and checkpoint each model after processing 50 mini-batches of size 128. All models are trained over 300 epochs using the SGD optimizer with an initial learning rate of 10^{-1} , a learning rate decay of 0.5 in 25 epoch increments, momentum 0.9, and weight decay 10^{-4} . To facilitate comparison with prior work, we match the accuracy of our models at the levels provided in Huang et al. (2020) (see Table 2 at 100% coverage for exact levels).

⁵<https://www.microsoft.com/en-us/download/details.aspx?id=54765>

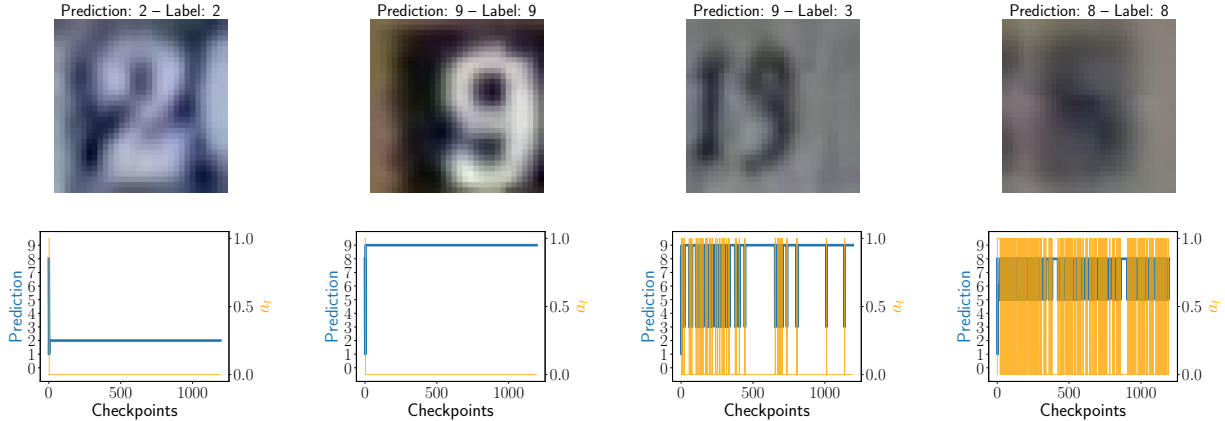


Figure 2: **Individual SVHN examples.** In the first row, we show four examples from the SVHN test set. For each example we plot both the prediction evolution and the final label agreement metric a_t over all checkpoints in the second row. We note that the first two examples are easy to classify as indicated by a mostly stationary prediction curve, while the last two examples are harder to classify since the prediction is highly unstable across intermediate models.

Baselines We compare our method based on neural network training dynamics (NNTD) to 5 common SC techniques previously introduced in § 2: Softmax Response (SR) (Geifman and El-Yaniv, 2017), SelectiveNet (SN) (Geifman and El-Yaniv, 2019), Deep Gamblers (DG) (Liu et al., 2019), Self-Adaptive Training (SAT) (Huang et al., 2020), and Monte-Carlo Dropout (MC-DO) (Gal and Ghahramani, 2016). We further compare against One-Sided Prediction (OSP) (Gangrade et al., 2021) in Appendix B.1. Our hyper-parameter tuning procedure for these baselines is documented in Appendix B.2.

4.2 Results

Our empirical results show that computing and thresholding the average score s_{avg} using weighting parameter $k = 0.05$ provides a strong score for selective classification. We denote this method $\text{NNTD}(s_{\text{avg}}, 0.05)$. In the following, we first study the accuracy/coverage trade-off with comparison to past work. Then, we present exemplary label evolution curves for individual SVHN examples. Finally, we analyze the performance of the metrics proposed in § 3 in depth and examine our method’s sensitivity to the checkpointing resolution and the weighting parameter k .

Accuracy/Coverage Trade-off Consistent with standard evaluation schemes for selective classification, our main experimental results examine the accuracy/coverage trade-off of $\text{NNTD}(s_{\text{avg}}, 0.05)$. We present our main performance results with comparison to past work in Tables 1 and 2 where we demonstrate NNTD’s effectiveness on CIFAR-10, SVHN, and Cats & Dogs. In Table 1, we document the results obtained by NNTD, SAT, SR, SN, DG, and MC-DO for a fixed low target error $e \in \{2\%, 1\%, 0.5\%\}$. In Table 2, we follow a similar setup but instead of fixing the target error we evaluate all methods for a fixed high target coverage $c \in \{100\%, 95\%, 90\%, 80\%, 70\%\}$. Across both experiments, we see that NNTD either matches or outperforms existing state-of-the-art selective classification methods.

Individual Evolution Plots To analyze the behavior of the metrics proposed in Section 3, we examine label prediction evolution curves for individual SVHN examples in Figure 2 (more examples provided in Appendix B.3). In particular, we select two easy-to-classify examples and two ambiguous examples from the test set and plot both the prediction evolution and the final label agreement metric a_t over all checkpoints. We observe that easy examples only show a small degree of oscillation while hard examples show more erratic patterns. This result matches our intuition: our model should produce correct decisions on data

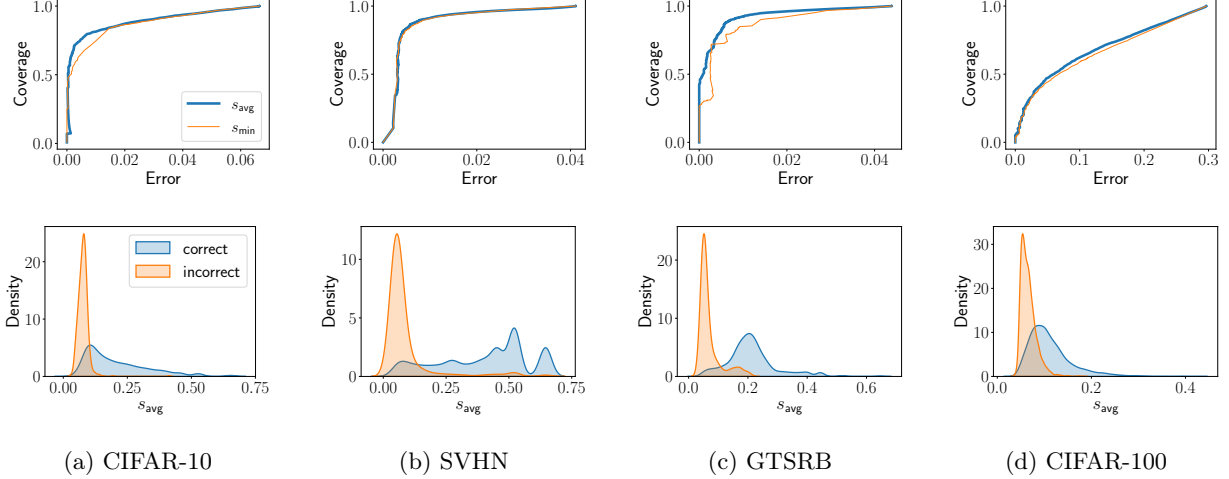


Figure 3: **Performance and distribution of our metrics for different datasets.** The first row shows the coverage/error curves for s_{\min} and s_{avg} . We show the distribution of the average score metric s_{avg} for both correctly and incorrectly classified samples in the second row.

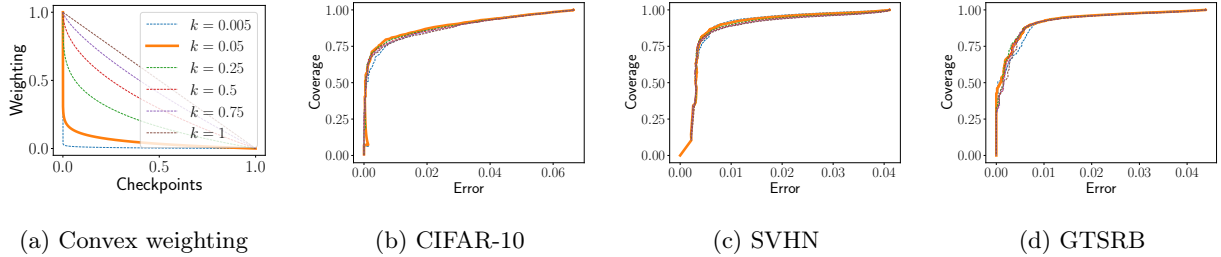


Figure 4: **Convex weighting used in $v_t = 1 - t^k$.** Overall, we find that $\text{NNTD}(s_{\text{avg}}, k)$ is generally robust to the exact choice of k and $k = 0.05$ performs best across our experiments.

points whose prediction is mostly constant throughout training and should reject data points for which intermediate models predict inconsistently.

Choice of Metric As per our theoretical framework and intuition provided in § 3, the average score s_{avg} should offer the most competitive selective classification performance. We confirm this finding in Figure 3 where we plot the coverage/error curves for CIFAR-10, SVHN, GTSRB, and CIFAR-100 for both s_{\min} and s_{avg} . Overall, we find that the average score s_{avg} consistently outperforms the more noisy minimum score s_{\min} . We also show that s_{avg} yields distinct distributional patterns for both correctly and incorrectly classified points. This separation enables strong coverage/accuracy trade-offs via our thresholding procedure.

Checkpoint weighting sensitivity One important hyper-parameter of our method is the weighting of intermediate predictions. Recall from § 3 that NNTD makes use of a convex weighting function $v_t = 1 - t^k$. In Figure 4, we observe that $\text{NNTD}(s_{\text{avg}}, k)$ is generally robust to the exact choice of k and that $k = 0.05$ performs best. At the same time, we find that decreasing k too much leads to a decrease in coverage at fixed accuracy levels. This result confirms that (i) large parts of the training process contain valuable signals for selective classification; and that (ii) early label disagreements should be de-emphasized by our method.

Checkpoint resolution sensitivity The second important hyper-parameter of our method is the granularity of available checkpoints. We study the sensitivity of $\text{NNTD}(s_{\text{avg}}, 0.05)$ with respect to the checkpointing resolution in Figure 5. Our experiments demonstrate favorable coverage/error trade-offs starting at 25-

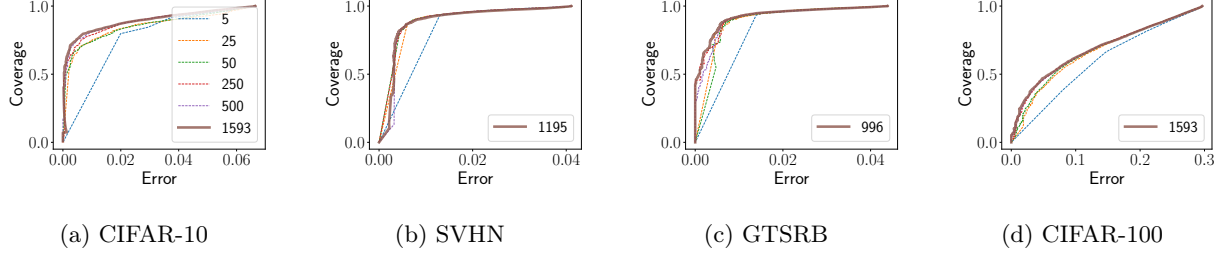


Figure 5: **Coverage/error trade-off of $\text{NNTD}(s_{\text{avg}}, 0.05)$ for various checkpointing resolutions.** Overall, we find that using 25-50 checkpoints already offers very competitive results. Using multiple hundreds of checkpoints offers diminishing returns but improves coverage at low error rates.

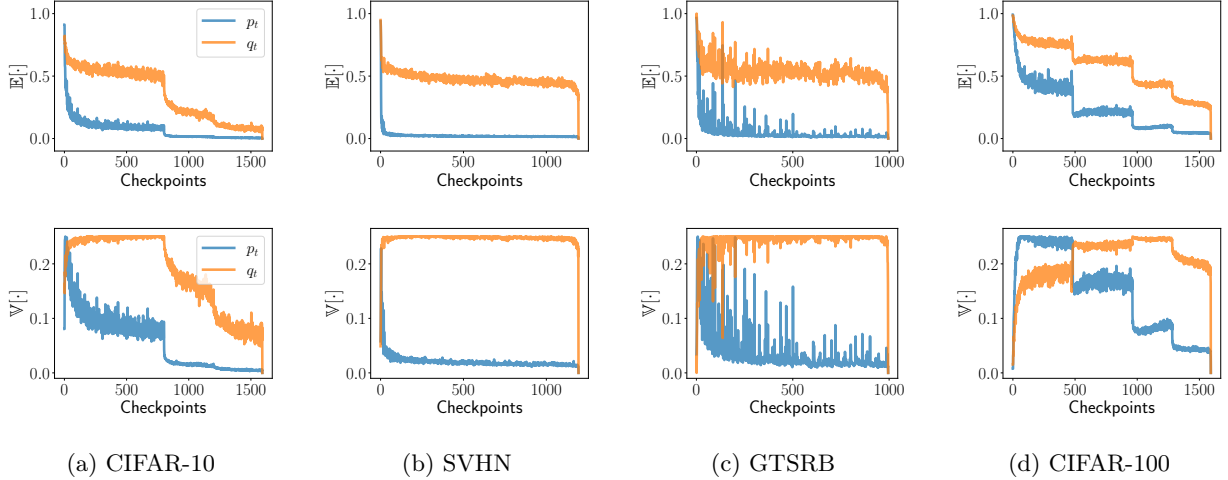


Figure 6: **Monitoring $\mathbb{E}[\cdot]$ and $\mathbb{V}[\cdot]$ for both correctly (p_t) and incorrectly (q_t) classified points.** Correctly classified points have both their expectations and variances quickly decreasing to 0 as training progresses. Incorrectly classified points both exhibit large expectations and variances and stay constant over large periods while training.

50 checkpoints. Further increasing the resolution to multiple hundreds of intermediate models does offer diminishing returns but also leads to better coverage especially at very low error rates.

4.3 Examining the Convergence Behavior of Correct & Incorrect Points

As alluded to in the assumptions presented in § 3.1, we empirically study how the label disagreement distributions over correctly classified data points (p_t) and incorrectly classified data points (q_t) evolve during training. From Figure 6 we observe that the expectations for correctly classified points are 0 for large time periods, with a sudden initial drop from near 1 to 0; this drop becomes elongated for more challenging data sets such as CIFAR-10 and CIFAR-100 (for which the learning rate scheduling is visible in the plot). We also see that the variances follow an analogous decreasing trend. In general, both $e_t = \mathbb{E}[p_t]$ and $v_t = \mathbb{V}[p_t]$ converge monotonically (and convexly) to 0. In contrast, incorrectly classified points show significantly larger mean and variance levels.

5 Discussion

We briefly discuss additional potential metric choices that we investigated but which lead to SC performance worse than s_{avg} . Note that a more elaborate discussion of these results is provided in Appendix B.3.

Incorporating Estimates of e_t into s_{\min} and s_{avg} Since the results in § 4.3 show that e_t is only nearly 0 almost everywhere, we investigate whether incorporating an estimate of e_t into s_{\min} and s_{avg} leads to additional SC improvements. Our results demonstrate that neither an empirical estimate nor a smooth decay function similar to v_t robustly improves over s_{\min} and s_{avg} (which assumed $e_t = 0$).

Jump Score s_{jmp} We also consider a score which captures the level of disagreement between the predicted label of two successive intermediate models (i.e., how much jumping occurred over the course of training). For $j_t = 0$ iff $f_t(\mathbf{x}) = f_{t-1}(\mathbf{x})$ and $j_t = 1$ otherwise we can compute the jump score as $s_{\text{jmp}} = 1 - \sum v_t j_t$ and threshold it as in § 3.2 and § 3.3.

Variance Score s_{var} for Continuous Metrics Finally, we consider monitoring the evolution of continuous metrics that have been shown to be correlated with example difficulty. More specifically, Jiang et al. (2020) show that the metric they propose for example difficulty is correlated with confidence and negative entropy. Moreover, they find that difficult examples (or challenging and underrepresented features) are learned later in the training process. This observation motivates designing a score based on these continuous metrics that penalises changes later in the training process more heavily. We consider the maximum softmax class probability known as confidence, the negative entropy and the gap between the most confident classes for each example instead of the model predictions. Assume that any of these metrics is given by a sequence $z = \{z_1, \dots, z_T\}$ obtained from T intermediate models. Then we can capture the uniformity of z via a (weighted) variance score $s_{\text{var}} = \sum_t w_t (z_t - \mu)^2$ for mean $\mu = \frac{1}{T} \sum_t z_t$ and an increasing weighting sequence $w = \{w_1, \dots, w_T\}$. We provide theoretical motivations for examining the variance of these continuous metrics in Appendix A.1 along with precise metric definitions.

6 Conclusion

We propose a new method to assess model outputs based on the training dynamics of the underlying ML model. Our approach is practical and can be directly implemented using existing checkpointing mechanisms. The method is non-intrusive, requires no changes to the standard model training, and either matches or significantly outperforms results obtained using previous techniques. Building on these foundations, future work could (i) investigate speeding up the inference procedure of intermediate models; (ii) study the existence of optimal weightings v_t ; or (iii) explore whether the NNTD framework can be applied to the related but distinct problem of out-of-distribution sample detection.

Acknowledgements

This work was supported by CIFAR (through a Canada CIFAR AI Chair), by NSERC (under the Discovery Program), and by a gift from Ericsson. We are also grateful to the Vector Institute’s sponsors for their financial support. In particular, we thank Roger Grosse, Chris Maddison, Franziska Boenisch, Natalie Dullerud, Jonas Guan, Michael Zhang, and Tom Ginsberg for fruitful discussions.

References

- Chirag Agarwal, Daniel D’souza, and Sara Hooker. Estimating example difficulty using variance of gradients. *arXiv preprint arXiv:2008.11600*, 2020.
- Robert Baldock, Hartmut Maennel, and Behnam Neyshabur. Deep learning through the lens of example difficulty. *Advances in Neural Information Processing Systems*, 34, 2021.
- Robert Challen, Joshua Denny, Martin Pitt, Luke Gompels, Tom Edwards, and Krasimira Tsaneva-Atanasova. Artificial intelligence, bias and clinical safety. *BMJ Quality & Safety*, 28(3):231–237, 2019.
- Haw-Shiuan Chang, Erik Learned-Miller, and Andrew McCallum. Active bias: Training more accurate neural networks by emphasizing high variance samples. *Advances in Neural Information Processing Systems*, 30, 2017.
- Ran El-Yaniv and Yair Wiener. On the foundations of noise-free selective classification. *Journal of Machine Learning Research*, 11(53):1605–1641, 2010. URL <http://jmlr.org/papers/v11/el-yaniv10a.html>.
- Vitaly Feldman and Chiyuan Zhang. What neural networks memorize and why: Discovering the long tail via influence estimation. *Advances in Neural Information Processing Systems*, 33:2881–2891, 2020.
- Jean Feng, Arjun Sondhi, Jessica Perry, and Noah Simon. Selective prediction-set models with coverage rate guarantees. *Biometrics*, 2021.
- Yarin Gal and Zoubin Ghahramani. Dropout as a bayesian approximation: Representing model uncertainty in deep learning. In *international conference on machine learning*, pages 1050–1059. PMLR, 2016.
- Aditya Gangrade, Anil Kag, and Venkatesh Saligrama. Selective classification via one-sided prediction. In *International Conference on Artificial Intelligence and Statistics*, pages 2179–2187. PMLR, 2021.
- Yonatan Geifman and Ran El-Yaniv. Selective classification for deep neural networks. *Advances in neural information processing systems*, 30, 2017.
- Yonatan Geifman and Ran El-Yaniv. Selectivenet: A deep neural network with an integrated reject option. In *International Conference on Machine Learning*, pages 2151–2159. PMLR, 2019.
- Yonatan Geifman, Guy Uziel, and Ran El-Yaniv. Bias-reduced uncertainty estimation for deep neural classifiers. *arXiv preprint arXiv:1805.08206*, 2018.
- Zahra Ghodsi, Siva Kumar Sastry Hari, Iuri Frosio, Timothy Tsai, Alejandro Troccoli, Stephen W Keckler, Siddharth Garg, and Anima Anandkumar. Generating and characterizing scenarios for safety testing of autonomous vehicles. *arXiv preprint arXiv:2103.07403*, 2021.
- Chuan Guo, Geoff Pleiss, Yu Sun, and Kilian Q Weinberger. On calibration of modern neural networks. In *International Conference on Machine Learning*, pages 1321–1330. PMLR, 2017.
- Kaiming He, Xiangyu Zhang, Shaoqing Ren, and Jian Sun. Deep residual learning for image recognition. In *Proceedings of the IEEE conference on computer vision and pattern recognition*, pages 770–778, 2016.
- Sara Hooker, Aaron Courville, Gregory Clark, Yann Dauphin, and Andrea Frome. What do compressed deep neural networks forget? *arXiv preprint arXiv:1911.05248*, 2019.
- Sebastian Houben, Johannes Stallkamp, Jan Salmen, Marc Schlipsing, and Christian Igel. Detection of traffic signs in real-world images: The German Traffic Sign Detection Benchmark. In *International Joint Conference on Neural Networks*, number 1288, 2013.
- Lang Huang, Chao Zhang, and Hongyang Zhang. Self-adaptive training: beyond empirical risk minimization. *Advances in neural information processing systems*, 33:19365–19376, 2020.
- Ziheng Jiang, Chiyuan Zhang, Kunal Talwar, and Michael C Mozer. Characterizing structural regularities of labeled data in overparameterized models. *arXiv preprint arXiv:2002.03206*, 2020.
- Erik Jones, Shiori Sagawa, Pang Wei Koh, Ananya Kumar, and Percy Liang. Selective classification can magnify disparities across groups. *arXiv preprint arXiv:2010.14134*, 2020.
- Fereshte Khani, Martin Rinard, and Percy Liang. Unanimous prediction for 100% precision with application

- to learning semantic mappings. *arXiv preprint arXiv:1606.06368*, 2016.
- Alex Krizhevsky, Geoffrey Hinton, et al. Learning multiple layers of features from tiny images. 2009.
- Balaji Lakshminarayanan, Alexander Pritzel, and Charles Blundell. Simple and scalable predictive uncertainty estimation using deep ensembles. In I. Guyon, U. Von Luxburg, S. Bengio, H. Wallach, R. Fergus, S. Vishwanathan, and R. Garnett, editors, *Advances in Neural Information Processing Systems*, volume 30. Curran Associates, Inc., 2017. URL <https://proceedings.neurips.cc/paper/2017/file/9ef2ed4b7fd2c810847ffa5fa85bce38-Paper.pdf>.
- Kimin Lee, Kibok Lee, Honglak Lee, and Jinwoo Shin. A simple unified framework for detecting out-of-distribution samples and adversarial attacks. *Advances in neural information processing systems*, 31, 2018.
- Shiyu Liang, Yixuan Li, and Rayadurgam Srikant. Enhancing the reliability of out-of-distribution image detection in neural networks. *arXiv preprint arXiv:1706.02690*, 2017.
- Weitang Liu, Xiaoyun Wang, John Owens, and Yixuan Li. Energy-based out-of-distribution detection. *Advances in Neural Information Processing Systems*, 33:21464–21475, 2020.
- Ziyin Liu, Zhikang Wang, Paul Pu Liang, Russ R Salakhutdinov, Louis-Philippe Morency, and Masahito Ueda. Deep gamblers: Learning to abstain with portfolio theory. *Advances in Neural Information Processing Systems*, 32, 2019.
- Hussein Mozannar and David Sontag. Consistent estimators for learning to defer to an expert. In *International Conference on Machine Learning*, pages 7076–7087. PMLR, 2020.
- Yuval Netzer, Tao Wang, Adam Coates, Alessandro Bissacco, Bo Wu, and Andrew Y Ng. Reading digits in natural images with unsupervised feature learning. 2011.
- Amir Mahdi Sadeghzadeh, Amir Mohammad Sobhanian, Faezeh Dehghan, and Rasool Jalili. Hoda: Hardness-oriented detection of model extraction attacks, 2021. URL <https://arxiv.org/abs/2106.11424>.
- Andrew I Schein and Lyle H Ungar. Active learning for logistic regression: an evaluation. *Machine Learning*, 68(3):235–265, 2007.
- Karen Simonyan and Andrew Zisserman. Very deep convolutional networks for large-scale image recognition. *arXiv preprint arXiv:1409.1556*, 2014.
- Mariya Toneva, Alessandro Sordoni, Remi Tachet des Combes, Adam Trischler, Yoshua Bengio, and Geoffrey J Gordon. An empirical study of example forgetting during deep neural network learning. *arXiv preprint arXiv:1812.05159*, 2018.
- Lucas Nunes Vieira, Minako O’Hagan, and Carol O’Sullivan. Understanding the societal impacts of machine translation: a critical review of the literature on medical and legal use cases. *Information, Communication & Society*, 24(11):1515–1532, 2021.

A Additional Theoretical Insights

A.1 Variance of Confidence in Logistic Regression

In order to show the effectiveness of the variance score s_{var} for continuous metrics, we provide a simple bound on the variance of confidence $\max_{y \in \mathcal{Y}} f_t(\mathbf{x})$ in the final checkpoints of the training. Assuming that the model has converged to a local minima with a low learning rate, we can assume that the distribution of model weights can be approximated by a Gaussian distribution.

We consider a linear regression problem where the inputs are linearly separable.

Lemma 2. *Assume that we have some Gaussian prior on the model parameters in the logistic regression setting across m final checkpoints. More specifically, given T total checkpoints of model parameters $\{\mathbf{w}_1, \mathbf{w}_2, \dots, \mathbf{w}_T\}$ we have $p(W = \mathbf{w}_t) = \mathcal{N}(\mathbf{w}_0 \mid \boldsymbol{\mu}, s\mathbf{I})$ for $t \in \{T - m + 1, \dots, T\}$ and we assume that final checkpoints of the model are sampled from this distribution. We show that the variance of model confidence $\max_{y \in \{-1, 1\}} p(y \mid \mathbf{x}_i, \mathbf{w}_t)$ for a datapoint (\mathbf{x}_i, y_i) can be upper bounded by a factor of probability of correctly classifying this example by the optimal weights.*

Proof. We first compute the variance of model predictions $p(y_i \mid \mathbf{x}_i, W)$ for a given datapoint (\mathbf{x}_i, y_i) . Following previous work (Schein and Ungar, 2007; Chang et al., 2017), the variance of predictions over these checkpoints can be estimated as follows:

Taking two terms in Taylor expansion for model predictions we have $p(y_i \mid \mathbf{x}_i, W) \simeq p(y_i \mid \mathbf{x}_i, \mathbf{w}) + g_i(\mathbf{w})^\top (W - \mathbf{w})$ where W and \mathbf{w} are current and the expected estimate of the parameters and $g_i(\mathbf{w}) = p(y_i \mid \mathbf{x}_i, \mathbf{w})(1 - p(y_i \mid \mathbf{x}_i, \mathbf{w}))\mathbf{x}_i$ is the gradient vector. Now we can write the variance with respect to the model prior as:

$$\mathbb{V}(p(y_i \mid \mathbf{x}_i, W)) \simeq \mathbb{V}(g_i(\mathbf{w})^\top (W - \mathbf{w})) = g_i(\mathbf{w})^\top F^{-1} g_i(\mathbf{w})$$

where F is the variance of posterior distribution $p(W \mid X, Y) \sim \mathcal{N}(W \mid \mathbf{w}, F^{-1})$. This suggests that the variance of probability of correctly classifying \mathbf{x}_i is proportional to $p(y_i \mid \mathbf{x}_i, \mathbf{w})^2(1 - p(y_i \mid \mathbf{x}_i, \mathbf{w}))^2$. Now we can bound the variance of maximum class probability or confidence as below:

$$\begin{aligned} \mathbb{V}\left(\max_{y \in \{-1, 1\}} p(y \mid \mathbf{x}_i, W)\right) &\leq \mathbb{V}(p(y_i \mid \mathbf{x}_i, W)) + \mathbb{V}(p(-y_i \mid \mathbf{x}_i, W)) \\ &\approx 2p(y_i \mid \mathbf{x}_i, \mathbf{w})^2(1 - p(y_i \mid \mathbf{x}_i, \mathbf{w}))^2 \mathbf{x}_i^\top F^{-1} \mathbf{x}_i \end{aligned}$$

□

We showed that if the probability of correctly classifying an example given the final estimate of model parameters is close to one, the variance of model predictions following a Gaussian Prior gets close to zero, we expect a similar behaviour for the variance of confidence under samples of this distribution.

B Extension of Empirical Evaluation

B.1 Comparison with One-Sided Prediction

In addition to the main results, we also compare NNTD to one-sided prediction (OSP). For this set of experiments, we evaluate our proposed approach on image dataset benchmarks that are common in the selective classification literature: CIFAR-10, SVHN, and Cats & Dogs. For each dataset, we train a deep neural network following the ResNet-32 architecture (He et al., 2016) and checkpoint each model after processing 50 mini-batches of size 128. All models are trained over 200 epochs. SVHN, Cats & Dogs, and GTSRB are trained using the Adam optimizer with learning rate 10^{-3} . The CIFAR-10 and CIFAR-100 models are trained using momentum-based stochastic gradient descent with an initial learning rate of 10^{-1} on a multi-step learning rate reduction schedule (reduction by 10^{-1} after epochs 100 and 150), momentum 0.9, and weight decay 10^{-4} . We report these results in Tables 3 and 4.

Table 3: **Performance at low target errors for OSP based setup.** Our $\text{NNTD}(s_{\text{avg}}, 0.05)$ method either matches or provides higher coverage levels of the test set at a fixed target error than other competing methods. Bold entries are within one standard deviation of each other over 5 random runs.

Dataset	Target Error	NNTD		OSP		SR		SN		DG	
		Cov.	Error	Cov.	Error	Cov.	Error	Cov.	Error	Cov.	Error
CIFAR-10	2%	83.3	1.96	80.6	1.91	75.1	2.09	73.0	2.31	74.2	1.98
	1%	79.7	1.05	74.0	1.02	67.2	1.09	64.5	1.02	66.4	1.01
	0.5%	74.2	0.49	64.1	0.51	59.3	0.53	57.6	0.48	57.8	0.51
SVHN	2%	95.7	1.96	95.8	1.99	95.7	2.06	93.5	2.03	94.8	1.99
	1%	91.2	0.99	90.1	1.03	88.4	0.99	86.5	1.04	89.5	1.01
	0.5%	83.9	0.50	82.4	0.51	77.3	0.51	79.2	0.51	81.6	0.49
Cats & Dogs	2%	90.5	2.03	90.5	1.98	88.2	2.03	84.3	1.94	87.4	1.94
	1%	85.6	1.01	85.4	0.98	80.2	0.97	78.0	0.98	81.7	0.98
	0.5%	77.5	0.50	78.7	0.49	73.2	0.49	70.5	0.46	74.5	0.48

Table 4: **Performance at high target coverage for OSP based setup.** Similar as demonstrated in Table 3, $\text{NNTD}(s_{\text{avg}}, 0.05)$ matches or outperforms state-of-the-art error rates at fixed coverage levels.

Dataset	Target Coverage	NNTD		OSP		SR		SN		DG	
		Cov.	Error	Cov.	Error	Cov.	Error	Cov.	Error	Cov.	Error
CIFAR-10	100%	100	9.57	100	9.74	99.99	9.58	100	11.07	100	10.81
	95%	95.1	6.13	95.1	6.98	95.2	8.74	94.7	8.34	95.1	8.21
	90%	90.1	4.16	90.0	4.67	90.5	6.52	89.6	6.45	90.1	6.14
SVHN	100%	100	4.11	100	4.27	99.97	3.86	100	4.27	100	4.03
	95%	94.8	1.80	95.1	1.83	95.1	1.86	95.1	2.53	95.0	2.05
	90%	90.1	0.77	90.1	1.01	90.0	1.04	90.1	1.31	90.0	1.06
Cats & Dogs	100%	100	5.18	100	5.93	100	5.72	100	7.36	100	6.16
	95%	94.9	2.99	95.1	2.97	95.0	3.46	95.2	5.1	95.1	4.28
	90%	90.0	1.87	90.0	1.74	90.0	2.28	90.2	3.3	90.0	2.50

B.2 Full Hyper-Parameters

We document full hyper-parameter settings for our method (NNTD) as well as all baseline approaches in Table 5. Baseline hyper-parameters are consistent with Gangrade et al. (2021) in the OSP setting and follow the setup from Huang et al. (2020) (Appendix A.4) for our main set of experiments.

B.3 Additional Selective Classification Results

B.3.1 Variance Score Experiments on Continuous Metrics

In addition to the evolution of predictions made across intermediate models, we also monitor a variety of easily computable continuous metrics. In our work, we consider the following metrics:

- Confidence (conf): $\max_{c \in \mathcal{Y}} f_t(\mathbf{x})$
- Confidence gap between top 2 most confident classes (gap): $\max_{c \in \mathcal{Y}} f_t(\mathbf{x}) - \max_{c \neq \hat{y}} f_t(\mathbf{x})$
- Entropy (ent): $-\sum_{c=1}^C f_t(\mathbf{x})_c \log(f_t(\mathbf{x})_c)$

Note that for the purpose of this experiment, we adapt the notation of f to map to a softmax-parameterized output instead of the hard thresholded label, formally $f: \mathcal{X} \rightarrow \mathbb{R}^{|\mathcal{Y}|}$.

We depict example evolution plots for these metrics in Figures 7, 8, 9, 10, and 11 in the third row.

Table 5: Hyper-parameters used for all SC algorithms in the OSP setup.

Dataset	SC Algorithm	Hyper-Parameters
CIFAR-10	Softmax Response (SR)	$t = 0.0445$
	Selective Net (SN)	$\lambda = 32, c = 0.51, t = 0.24$
	Deep Gamblers (DG)	$o = 1.179, t = 0.03$
	One-Sided Prediction (OSP)	$\mu = 0.49, t = 0.8884$
	Neural Network Training Dynamics (NNTD)	$T = 1593, k = 0.05$
SVHN	Softmax Response (SR)	$t = 0.0224$
	Selective Net (SN)	$\lambda = 32, c = 0.79, t = 0.86$
	Deep Gamblers (DG)	$o = 1.13, t = 0.23$
	One-Sided Prediction (OSP)	$\mu = 1.67, t = 0.9762$
	Neural Network Training Dynamics (NNTD)	$T = 1195, k = 0.05$
Cats & Dogs	Softmax Response (SR)	$t = 0.029$
	Selective Net (SN)	$\lambda = 32, c = 0.7, t = 0.73$
	Deep Gamblers (DG)	$o = 1.34, t = 0.06$
	One-Sided Prediction (OSP)	$\mu = 1.67, t = 0.9532$
	Neural Network Training Dynamics (NNTD)	$T = 797, k = 0.05$

B.3.2 Individual Metric Evolution Plots

We provide additional individual metric evolution plots for SVHN (Figure 7), GTSRB (Figure 8), CIFAR-10 (Figure 9), CIFAR-100 (Figure 10), and Cats & Dogs (Figure 11).

B.3.3 Incorporating Estimates of e_t into s_{\min} and s_{avg}

Our results in § 4.3 show that e_t is only nearly 0 almost everywhere, we investigate whether incorporating an estimate of e_t into s_{\min} and s_{avg} leads to additional SC improvements. Recall that in Lemma 1 we gave an upper-bound on the probability that the test point is correctly classified as $\frac{v_t}{|a_t - e_t|^2}$. In the case where e_t is not 0 everywhere, we can adjust

$$s_{\min} = \min_{t \text{ s.t. } a_t=1} \frac{v_t}{|a_t - e_t|^2} \quad \text{and} \quad s_{\text{avg}} = \frac{\sum \frac{v_t}{|a_t - e_t|^2} a_t}{\sum a_t} \quad (3)$$

accordingly. In Figure 12, we experimentally test whether incorporating an empirical estimate (first row) or a smooth decay function similar to v_i (second row) robustly improve over s_{\min} and s_{avg} with $e_t = 0$. Our results show that neither setting outperforms our default setting with $e_t = 0$.

B.3.4 Performance of Jump Score s_{jump} and Weighted Variance s_{var}

As discussed in § 5, we also investigated whether the jump score s_{jump} or the weighted variance of continuous metrics s_{var} can be used as an effective score for SC. As we show in Figure 13, none of these metrics robustly outperforms our main method $\text{NNTD}(s_{\text{avg}}, 0.05)$.

B.3.5 Concave Weighting for v_t

As we have empirically analyzed in § 4.3, the variances v_t follow a monotonically decreasing and convex trend. This inspires our best performing method $\text{NNTD}(s_{\text{avg}}, 0.05)$ to use $k = 0.05$ for $v_i = 1 - i^k$. As a sanity check, we examine whether a concave weighting yielded by $v_i = 1 - i^k$ for $k \geq 1$. As we demonstrate in Figure 14, the best concave weighting is given by $k = 1$. Therefore, we confirm that no concave weighting outperforms the convex weightings analyzed in Figure 4.

Table 6: **Coverage/Error trade-off of NNTD as a function of the accounted data points (CIFAR-10 left, SVHN right).** We observe that large parts of the training process contain valuable signals for selective classification.

Target Coverage	100%	90%	80%	50%	20%	10%
100%	6.07	6.08	6.10	6.15	6.18	6.20
95%	3.24	3.25	3.25	3.31	3.34	3.39
90%	1.83	1.83	1.84	1.88	1.91	1.93
80%	0.64	0.65	0.67	0.72	0.78	0.79
70%	0.34	0.34	0.36	0.38	0.40	0.40

Target Coverage	100%	90%	80%	50%	20%	10%
100%	2.68	2.70	2.73	2.83	2.88	2.92
95%	0.88	0.90	0.93	1.01	1.09	1.11
90%	0.55	0.57	0.59	0.62	0.68	0.73
80%	0.38	0.39	0.40	0.45	0.51	0.53
70%	0.33	0.33	0.35	0.41	0.44	0.45

B.3.6 Limiting NNTD to a Subset of Last Checkpoints

In order to determine which training stages are important for selective classification, we perform an experiment on CIFAR-10 and SVHN where we limit ourselves to a subset of the last checkpoints. In particular, we examine the coverage/error trade-off for only including the last $\{10\%, 20\%, 50\%, 80\%, 90\%, 100\%\}$ of checkpoints. We report our findings in Table 6. We see that taking into account more than 80% of checkpoints does lead to diminishing returns and that only taking into account 50% or less of the total numbers of checkpoints does not lead to state-of-the-art selective classification performance.

B.3.7 Selective Classification on ImageNet

In addition to our main results on CIFAR-10, CIFAR-100, SVHN, Cats & Dogs, and GTSRB, we also provide results for our NNTD approach on ImageNet. We train a ResNet-50 over 90 epochs with an initial learning rate of 0.1, a learning rate decay of 0.1 in 30 epoch increments, momentum 0.9, and weight decay 10^{-4} . We report our obtained accuracy/coverage trade-off in Table 7 and find that NNTD delivers a strong coverage/error trade-off compared to the softmax response and self-adaptive training baselines.

B.3.8 Applying OOD Scores to Selective Classification

Finally, we also compare popular out-of-distribution detection approaches to our NNTD method. In particular, we apply three state-of-the-art approaches, namely energy-based OOD detection (**Energy**) (Liu et al., 2020), Mahalanobis-distance-based OOD detection (**Mahalanobis**) (Lee et al., 2018), and ODIN (ODIN) (Liang et al., 2017) to the CIFAR-10 and SVHN test sets and document these results in Table 8. Overall, we find that SOTA out-of-distribution detection techniques are not well equipped to attain SOTA selective classification performance; NNTD outperforms these methods by a large margin.

C Broader Impact Statement

Modern neural networks often produce overconfident decisions (Guo et al., 2017). This limitation, amongst other shortcomings, prevents neural nets from being readily applied in high-stakes decision-making. Selective classification is one paradigm enabling the rejection of data points. In particular, samples that would most likely be misclassified should be rejected. Since our work improves over current state-of-the-art methods, our work can be used to enhance the trustworthiness of deep neural networks in practice. While modern selective classification techniques mitigates overconfidence, recent work has also shown that SC algorithms disproportionately reject samples from minority groups (Jones et al., 2020). This finding suggests that improvements to the overall coverage comes at a fairness cost. As a result, the connection between fairness and sample rejection still warrants further investigation.

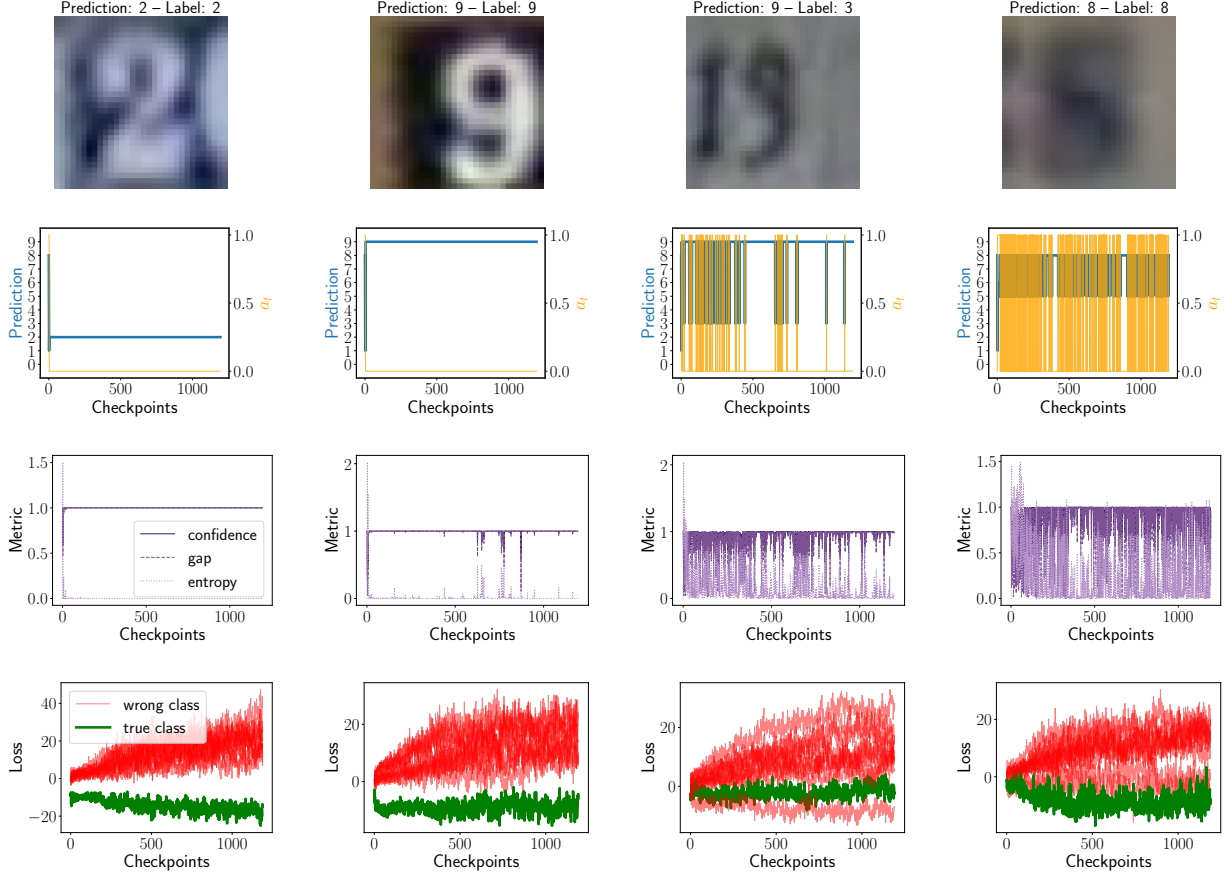


Figure 7: **Individual SVHN examples.** We extend Figure 2 by also including the evolution of the confidence, the gap, and the entropy over the course of training in the third row. In the final row, we further plot the loss evolution for all candidate classes. We note that the first two examples are easy to classify as indicated by mostly stationary metrics and a clear loss separation, while the last two examples are harder to classify since they exhibit highly erratic metrics and ambiguous loss curves.

Table 7: **ImageNet coverage/error results.** We observe that NNTD outperforms the SR baseline by a large margin and offers comparable performance as SAT.

Target	NNTD		SAT		SR	
Error	Cov \uparrow	Err	Cov \uparrow	Err	Cov \uparrow	Err
10%	54.4	10.0	53.7	10.0	15.2	10.0
5%	26.3	5.0	25.8	5.0	5.4	5.0
2%	8.1	2.0	8.8	2.0	1.1	2.0
1%	3.6	1.0	4.0	1.8	0.7	1.8
0.5%	2.3	0.7	2.2	0.6	0.0	0.0

Target	NNTD		SAT		SR	
Coverage	Cov	Err \downarrow	Cov	Err \downarrow	Cov	Err \downarrow
100%	100	24.2	100	24.2	100	24.2
95%	95.0	23.2	95.0	22.8	95.0	23.5
90%	90.0	22.5	90.0	22.6	90.0	22.9
80%	80.0	18.0	80.0	18.4	80.0	21.7
70%	70.0	14.1	70.0	14.3	70.0	20.7

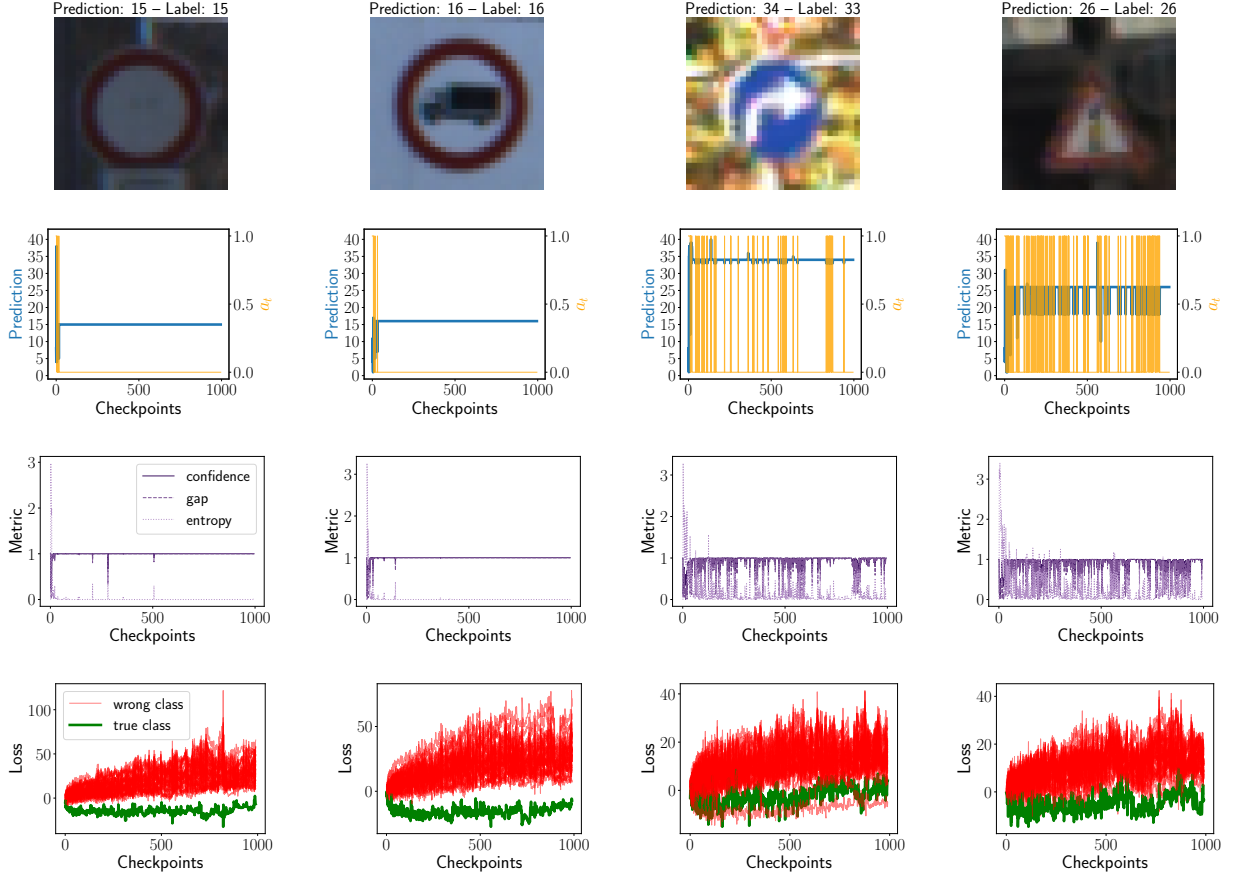


Figure 8: **Individual GTSRB examples.** Similar as Figure 7.

Table 8: **Performance of NNTD in comparison with OOD scores.** We find that NNTD significantly outperforms common OOD detection approaches for the purpose of selective classification.

Dataset	Target	NNTD		Energy		Mahalanobis		ODIN	
		Coverage	Cov	Err ↓	Cov	Err ↓	Cov	Err ↓	Cov
CIFAR-10	100%	100	6.07	100	6.07	100	6.07	100	6.07
	95%	95.0	3.24	95.0	3.99	95.0	4.44	95.1	6.04
	90%	90.1	1.83	90.0	2.67	90.0	2.93	88.9	6.01
	80%	79.9	0.64	80.0	1.10	80.1	1.20	88.9	6.01
	70%	69.8	0.34	70.0	0.83	69.9	0.82	68.3	4.41
SVHN	100%	100	2.68	100	2.68	100	2.68	100	2.68
	95%	95.0	0.88	95.1	1.35	95.1	1.51	95.0	2.67
	90%	90.1	0.55	89.9	0.92	90.0	1.04	89.9	2.64
	80%	79.9	0.38	79.9	0.70	80.3	0.70	81.9	2.51
	70%	69.8	0.33	70.0	0.58	69.8	0.58	74.9	2.18

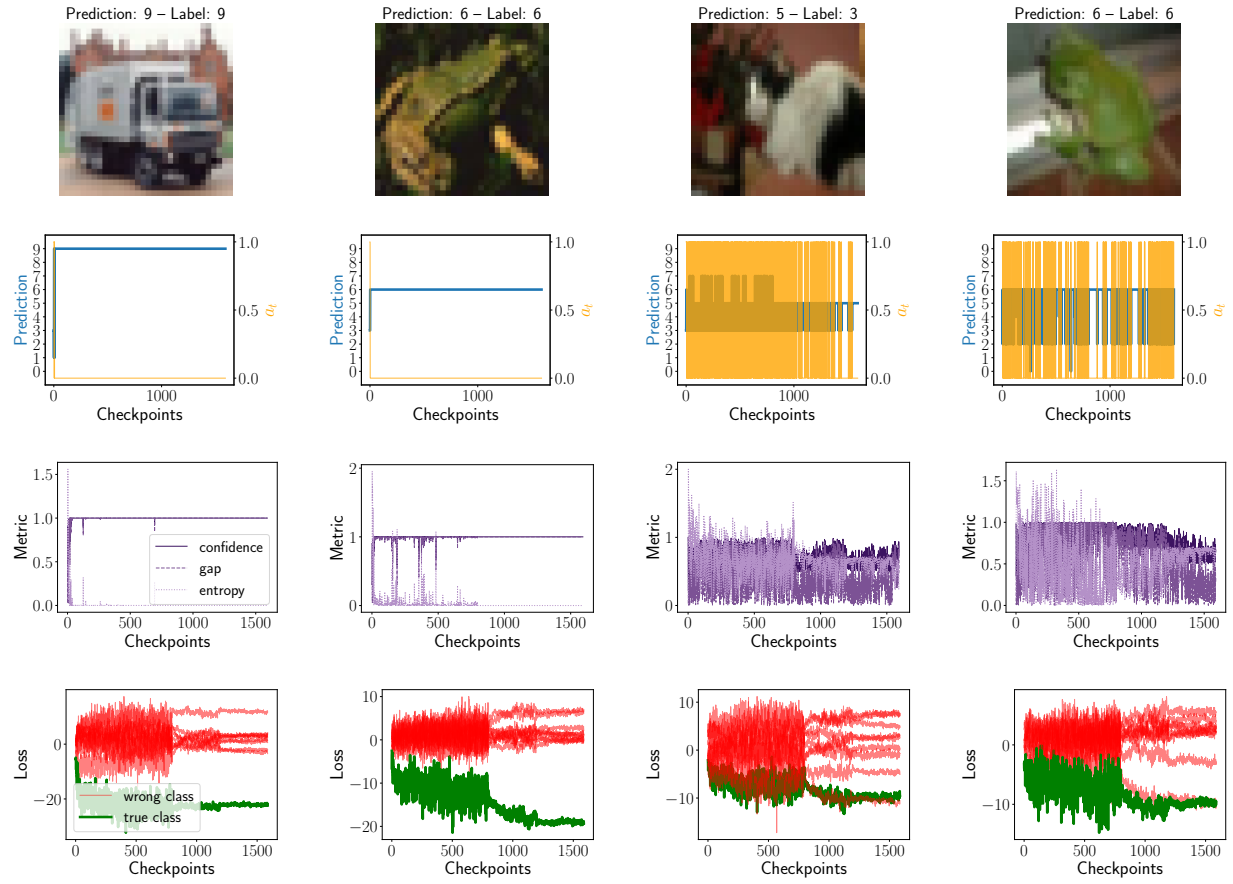


Figure 9: **Individual CIFAR-10 examples.** Similar as Figure 7.

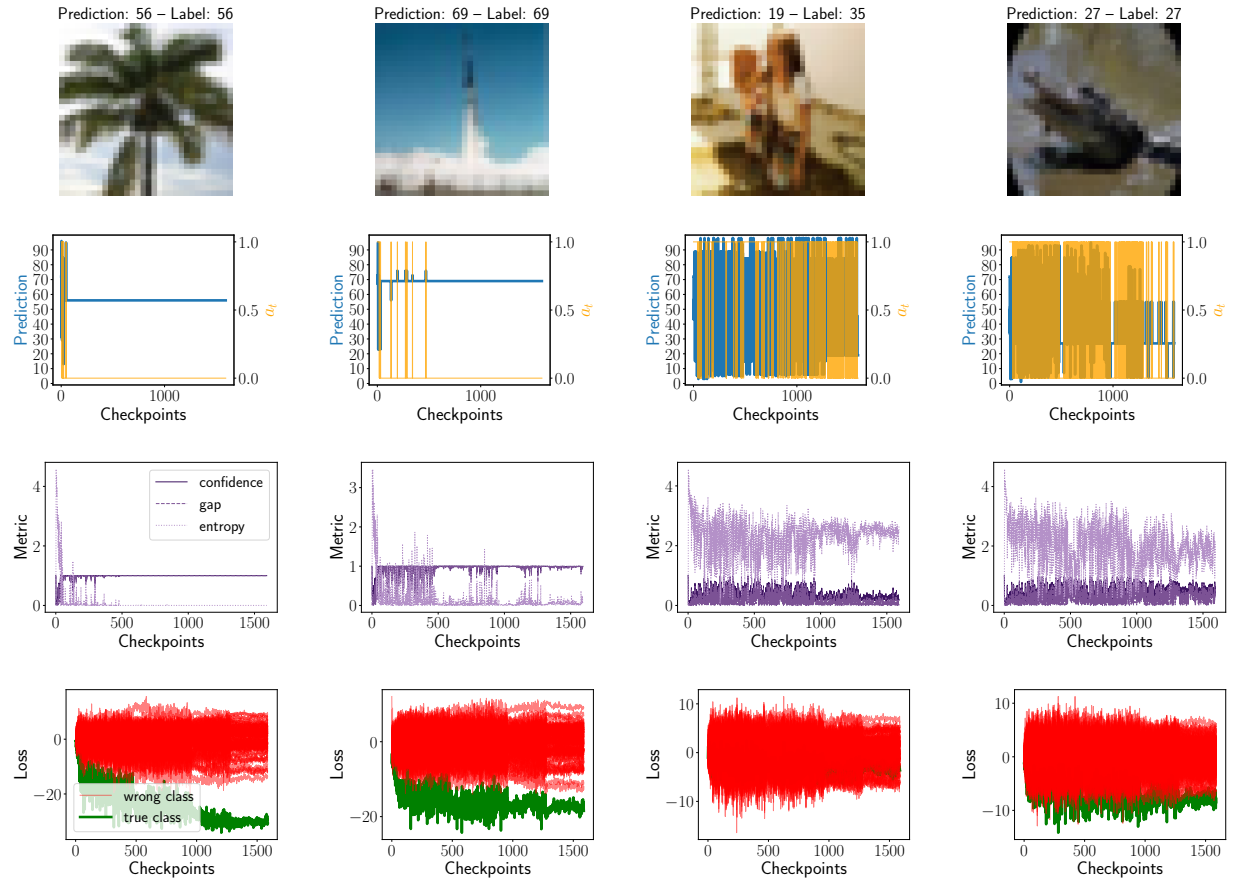


Figure 10: **Individual CIFAR-100 examples.** Similar as Figure 7.

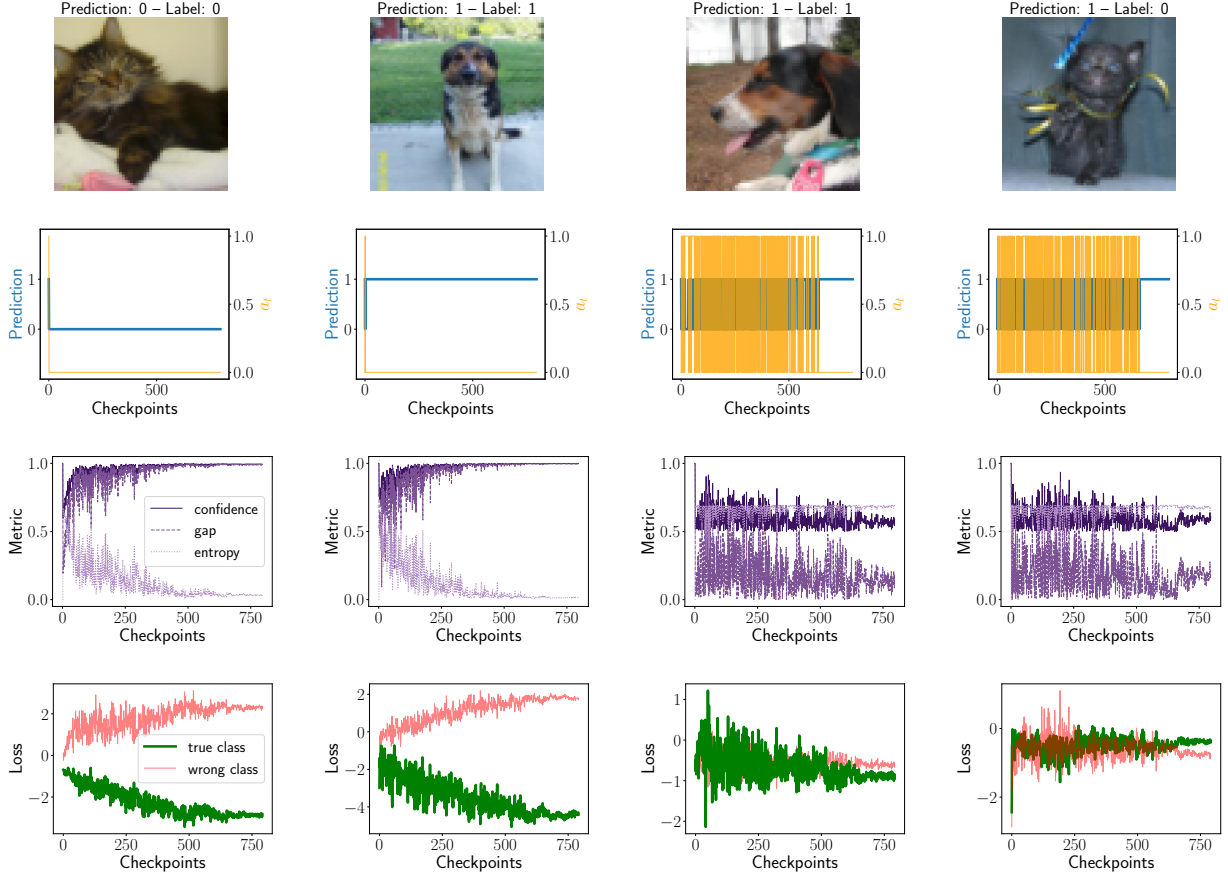


Figure 11: Individual Cats & Dogs examples. Similar as Figure 7.

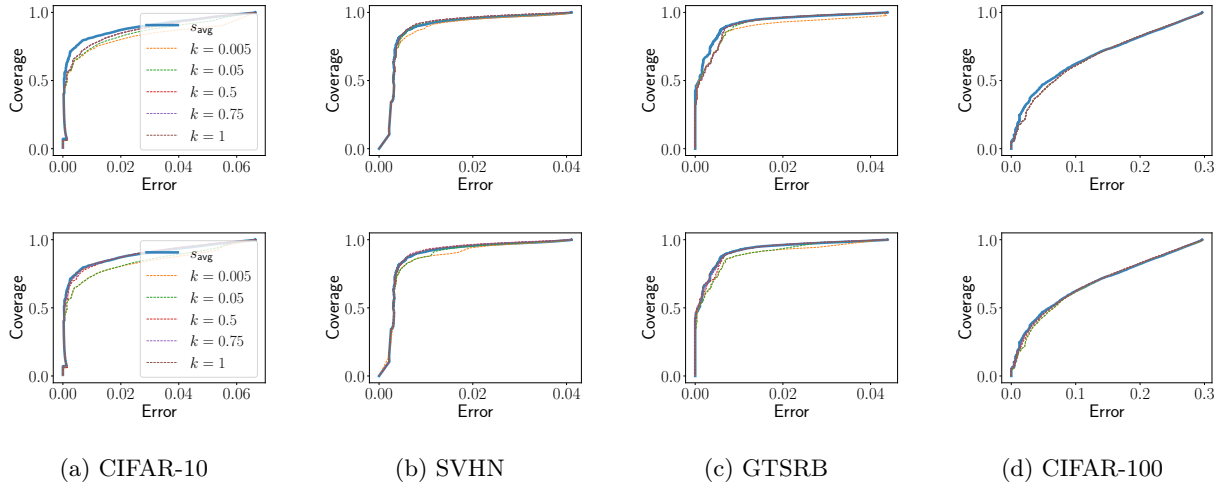


Figure 12: **Coverage/error trade-off when incorporating e_t into s_{\min} and s_{avg} .** In the first row, the solid blue line corresponds to $\text{NTND}(s_{\text{avg}}, 0.05)$ while the dashed lines show the performance when we incorporate an empirical estimate of e_t for various weightings v_i . In the second row, maintaining the solid blue line as $\text{NTND}(s_{\text{avg}}, 0.05)$, we fix v_t at $k = 0.05$ and test various continuous approximations of e_t as $e_t = 1 - t^k$ for $k \in (0, 1]$. Overall, we find that introducing an adaptable e_t does not further improve the performance of s_{\min} and s_{avg} with $e_t = 0$.

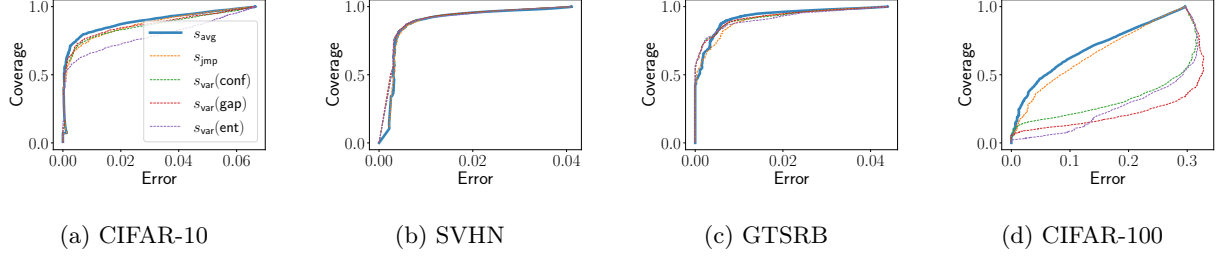


Figure 13: **Coverage/error trade-off of NNTD for alternate scores.** We find that neither the jump score, nor any of the weighted variance metrics at their optimal k for v_i outperform $\text{NNTD}(s_{\text{avg}}, 0.05)$.

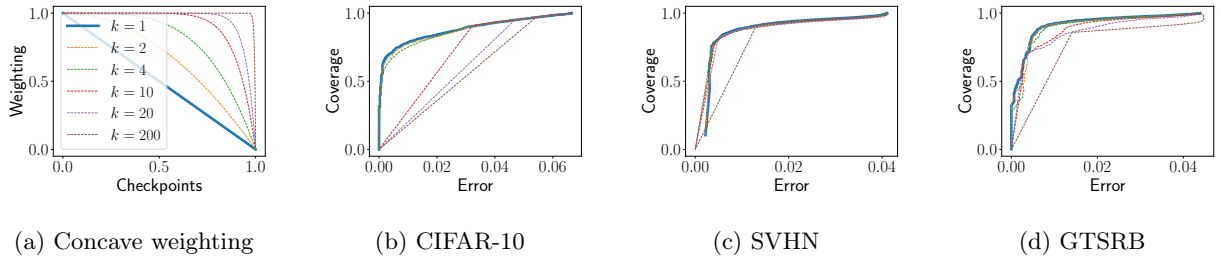


Figure 14: **Concave weighting used in $v_t = 1 - t^k$.** Overall, since the best concave weighting is given by $k = 1$, we conclude that no concave weighting outperforms any convex weighting.

Table 9: Performance at low target errors. Same results as in Table 1 but includes standard deviations.

Dataset	Target Error	MTD			SAT			DG			SH			SR			MC-DG		
		Cov \uparrow	Err		Cov \uparrow	Err		Cov \uparrow	Err		Cov \uparrow	Err		Cov \uparrow	Err		Cov \uparrow	Err	
CIFAR-10	2%	91.2 (± 0.05)	1.99 (± 0.01)		90.3 (± 0.03)	1.97 (± 0.02)		89.1 (± 0.04)	2.02 (± 0.01)		88.3 (± 0.03)	2.03 (± 0.02)		85.8 (± 0.08)	1.98 (± 0.02)		86.1 (± 0.07)	2.01 (± 0.01)	
	1%	86.4 (± 0.03)	1.00 (± 0.01)		86.1 (± 0.02)	1.02 (± 0.02)		85.5 (± 0.07)	1.03 (± 0.02)		84.4 (± 0.06)	0.98 (± 0.06)		79.1 (± 0.08)	1.01 (± 0.03)		79.9 (± 0.08)	1.01 (± 0.03)	
	0.5%	75.9 (± 0.04)	0.49 (± 0.02)		76.0 (± 0.05)	0.51 (± 0.02)		75.2 (± 0.08)	0.5 (± 0.03)		74.7 (± 0.09)	0.49 (± 0.01)		71.2 (± 0.05)	0.51 (± 0.02)		72.0 (± 0.03)	0.50 (± 0.03)	
SVHN	2%	98.5 (± 0.05)	1.98 (± 0.03)		98.2 (± 0.04)	1.99 (± 0.02)		97.8 (± 0.03)	2.06 (± 0.05)		97.7 (± 0.06)	2.03 (± 0.02)		97.6 (± 0.05)	1.99 (± 0.03)		97.9 (± 0.03)	2.00 (± 0.04)	
	1%	96.3 (± 0.03)	0.99 (± 0.02)		95.7 (± 0.02)	1.03 (± 0.03)		94.8 (± 0.04)	0.99 (± 0.01)		94.5 (± 0.03)	1.04 (± 0.02)		93.5 (± 0.05)	1.01 (± 0.03)		94.1 (± 0.06)	0.97 (± 0.02)	
	0.5%	88.1 (± 0.02)	0.50 (± 0.02)		87.9 (± 0.05)	0.51 (± 0.01)		86.4 (± 0.04)	0.51 (± 0.01)		86.0 (± 0.04)	0.51 (± 0.01)		70.0 (± 0.09)	0.50 (± 0.04)		70.1 (± 0.04)	0.49 (± 0.03)	
Cats & Dogs	2%	97.7 (± 0.09)	2.01 (± 0.03)		98.2 (± 0.02)	1.98 (± 0.03)		98.0 (± 0.05)	2.03 (± 0.02)		97.4 (± 0.05)	1.98 (± 0.03)		95.1 (± 0.12)	1.99 (± 0.04)		95.7 (± 0.10)	1.99 (± 0.03)	
	1%	93.1 (± 0.03)	1.01 (± 0.02)		93.6 (± 0.02)	0.98 (± 0.03)		92.6 (± 0.08)	0.97 (± 0.04)		92.2 (± 0.05)	0.98 (± 0.02)		86.9 (± 0.13)	0.98 (± 0.04)		88.6 (± 0.09)	1.01 (± 0.02)	
	0.5%	85.7 (± 0.06)	0.51 (± 0.02)		86.0 (± 0.04)	0.49 (± 0.01)		85.3 (± 0.02)	0.49 (± 0.02)		84.8 (± 0.03)	0.46 (± 0.05)		68.4 (± 0.10)	0.48 (± 0.02)		70.1 (± 0.08)	0.51 (± 0.03)	

Table 10: Performance at high target coverage. Same results as in Table 2 but includes standard deviations.

Dataset	Target Coverage	BMTD			SAT			DG			SN			SR			MC-DD		
		Cov	Err ↓		Cov	Err ↓		Cov	Err ↓		Cov	Err ↓		Cov	Err ↓		Cov	Err ↓	
CIFAR-10	100%	100 (± 0.00)	6.07 (± 0.05)		100 (± 0.00)	6.06 (± 0.03)		100 (± 0.00)	6.11 (± 0.05)		100 (± 0.00)	6.13 (± 0.03)		100 (± 0.00)	6.13 (± 0.03)		100 (± 0.00)	6.13 (± 0.03)	
	95%	95.0 (± 0.01)	3.24 (± 0.03)		95.1 (± 0.01)	3.32 (± 0.05)		95.1 (± 0.02)	3.47 (± 0.06)		95.0 (± 0.01)	4.08 (± 0.08)		94.9 (± 0.03)	4.48 (± 0.07)		95.1 (± 0.04)	4.48 (± 0.09)	
	90%	90.1 (± 0.02)	1.83 (± 0.04)		89.9 (± 0.02)	1.90 (± 0.02)		90.0 (± 0.01)	2.19 (± 0.05)		90.1 (± 0.02)	2.29 (± 0.03)		90.1 (± 0.02)	2.78 (± 0.06)		90.0 (± 0.02)	2.87 (± 0.07)	
	80%	79.9 (± 0.02)	0.64 (± 0.03)		80.0 (± 0.00)	0.65 (± 0.04)		80.1 (± 0.03)	0.66 (± 0.04)		80.1 (± 0.01)	0.81 (± 0.07)		79.8 (± 0.02)	1.05 (± 0.08)		79.9 (± 0.01)	1.01 (± 0.03)	
SVHN	70%	69.8 (± 0.03)	0.34 (± 0.04)		69.9 (± 0.03)	0.32 (± 0.05)		69.8 (± 0.04)	0.41 (± 0.04)		70.2 (± 0.03)	0.30 (± 0.02)		70.0 (± 0.01)	0.47 (± 0.07)		70.1 (± 0.02)	0.42 (± 0.05)	
	100%	100 (± 0.00)	2.68 (± 0.02)		100 (± 0.00)	2.71 (± 0.03)		100 (± 0.00)	2.72 (± 0.05)		100 (± 0.00)	2.77 (± 0.06)		100 (± 0.00)	2.77 (± 0.06)		100 (± 0.00)	2.77 (± 0.06)	
	95%	95.0 (± 0.01)	0.88 (± 0.02)		95.1 (± 0.01)	0.95 (± 0.03)		95.1 (± 0.01)	1.01 (± 0.06)		95.0 (± 0.02)	1.07 (± 0.05)		94.9 (± 0.03)	1.15 (± 0.11)		95.1 (± 0.02)	1.12 (± 0.07)	
	90%	90.1 (± 0.02)	0.55 (± 0.4)		89.9 (± 0.01)	0.58 (± 0.01)		90.0 (± 0.00)	0.63 (± 0.06)		90.1 (± 0.01)	0.71 (± 0.04)		90.1 (± 0.02)	0.82 (± 0.06)		90.0 (± 0.02)	0.76 (± 0.03)	
Cats & Dogs	80%	79.9 (± 0.01)	0.38 (± 0.03)		80.0 (± 0.01)	0.37 (± 0.02)		80.1 (± 0.01)	0.43 (± 0.01)		80.1 (± 0.00)	0.48 (± 0.02)		79.8 (± 0.03)	0.55 (± 0.09)		79.9 (± 0.02)	0.53 (± 0.08)	
	70%	69.8 (± 0.03)	0.33 (± 0.03)		69.9 (± 0.02)	0.33 (± 0.01)		69.8 (± 0.04)	0.35 (± 0.02)		70.2 (± 0.02)	0.45 (± 0.06)		70.0 (± 0.01)	0.50 (± 0.05)		70.1 (± 0.02)	0.49 (± 0.06)	
	100%	100 (± 0.00)	3.48 (± 0.01)		100 (± 0.00)	3.45 (± 0.01)		100 (± 0.00)	3.41 (± 0.03)		100 (± 0.00)	3.56 (± 0.04)		100 (± 0.00)	3.56 (± 0.04)		100 (± 0.00)	3.56 (± 0.04)	
	95%	95.1 (± 0.02)	1.51 (± 0.03)		95.1 (± 0.03)	1.45 (± 0.02)		95.0 (± 0.01)	1.43 (± 0.02)		94.9 (± 0.02)	1.61 (± 0.05)		94.8 (± 0.03)	1.92 (± 0.12)		95.1 (± 0.02)	1.95 (± 0.08)	
Cats & Dogs	90%	90.1 (± 0.03)	0.60 (± 0.03)		89.9 (± 0.02)	0.57 (± 0.03)		90.0 (± 0.01)	0.69 (± 0.04)		90.1 (± 0.02)	0.95 (± 0.11)		90.1 (± 0.03)	1.13 (± 0.07)		90.0 (± 0.01)	1.09 (± 0.06)	
	80%	79.9 (± 0.01)	0.42 (± 0.04)		80.0 (± 0.01)	0.41 (± 0.03)		80.1 (± 0.02)	0.56 (± 0.02)		80.1 (± 0.03)	0.39 (± 0.05)		79.8 (± 0.02)	0.69 (± 0.07)		79.9 (± 0.02)	0.58 (± 0.05)	
	70%	69.8 (± 0.02)	0.36 (± 0.05)		69.9 (± 0.03)	0.33 (± 0.03)		69.8 (± 0.03)	0.45 (± 0.05)		70.2 (± 0.03)	0.33 (± 0.03)		70.0 (± 0.01)	0.62 (± 0.06)		70.1 (± 0.02)	0.51 (± 0.04)	